Engineering and Technology Journal
Journal homepage: https://etj.uotechnology.edu.iq

Investigation of Frequency-Domain-Based Vibration Signal Analysis for UAV Unbalance Fault Classification

Luttfi A. Al-Haddad[a,b]*, Alaa A. Jaber[b], Paramin Neranon[c], Sinan A. Al-Haddad[d]

[a]Training and Workshop Center, University of Technology-Iraq, Alsinaa Street 52, 10066 Baghdad, Iraq.
[b]Mechanical Engineering Department, University of Technology-Iraq, Alsinaa Street 52, 10066 Baghdad, Iraq.
[c]Department of Mechanical and Mechatronics Engineering, Faculty of Engineering, Prince of Songkla University, Songkhla 90112, Thailand.
[d]Civil Engineering Department, University of Technology-Iraq, Alsinaa Street 52, 10066 Baghdad, Iraq.
*Corresponding author Email: Luttfi.A.AlHaddad@uotechnology.edu.iq

HIGHLIGHTS

- Small UAV drone vibration signals are gathered utilizing the LabVIEW DAQ assistant.
- Spectral analysis of Fast Fourier Transform signal processing technique in x, y, and z was performed.
- Unbalance fault classification based on FFT peak frequencies of rolling, pitching, and yawing in a DJI mini 2 combo was used.
- Real-time UAV health monitoring method was discussed and explained accordingly.

ARTICLE INFO

Handling editor: Muhsin Jweeg

Keywords:
Signal Processing; Vibration Signal Analysis; Fast Fourier Transform; UAV; Unbalance Classification.

ABSTRACT

The flying reliability of Unmanned Aerial Vehicles (UAVs) and flying robots, which directly determines the operational degree of safety, is becoming more important in recent intelligent decades. Reliability and a high level of safety are critical for autonomously controlled flying robots, especially in transportation and entertainment applications. Subsequently, monitoring UAV health is crucial and essential for system safety, cost savings, and excellent dependability. The development of numerous monitoring strategies has resulted from the requirement for a simple and accurate unbalance classification procedure. This paper provides an Unbalance Classification and Isolation (UCI) system for multirotor UAV propeller impairments. The technique is based on the processing of signal vectors from a vibration sensor positioned in the lines of the intersection of a modern-day drone's four propulsion units, which supply data for the Fast Fourier Transform (FFT) feature extraction. To identify and locate broken blades, characteristic fault signatures collected from vibration signals are employed and displayed in real-time on the programming platform. A noticeable maximum frequency shifting percentage value of 4.2% is acquired when deviating from a healthy state. The results reveal that identifying and isolating defective rotor states has high sensitivity and outperforms current studies in regard to unbalance classification of UAVs. The adopted technique is an efficient and low-cost solution that can be implemented in any multirotor UAV.

1. Introduction

Unmanned Aerial Vehicles (UAVs) are a new technology that has the potential to be employed in a broad range of businesses and fields of human activity to offer a variety of services and operations. The growing popularity of small multirotor UAVs raises questions about their operational security and safety in a human-shared world. Even though mini-scale UAVs have several applications, such as civil security control, traffic monitoring, and environmental management, effective safety procedures are required for their pervasive functioning [1]. One potential solution is to use Unbalance Classification and Isolation (UCI) methodologies, which boost the dependability of mini-UAVs by assuring a minimum level of system performance under failure situations.

Rotor blades are the most critical components used in UAVs for balance, motion transmission, and propulsion (lifting force). The spinning motor of a mini-UAV system is typically connected to the housing of the drone system's frame, while the rotor blades rotate as the motor spins. Drone loads and vibrations are transmitted from the blades to the housing and structure through the drone system's connections. Furthermore, vibration analysis is often used to locate defects in rotating machinery and mini-UAVs. Many vibration signal analysis techniques have previously been applied to diagnose rotating machine defects [2,3,4]. Previous studies frequently employed offline condition monitoring and imbalance classification techniques, resulting in

http://doi.org/10.30684/etj.2023.137412.1348
Received 05 January 2023; Accepted 10 February 2023; Available online 23 February 2023
2412-0758/University of Technology-Iraq, Baghdad, Iraq

extended-time decisions. This may be unreliable since we sometimes require instant choices when time is limited. To classify unbalances and errors in a mini-UAV, a real-time condition monitoring and decision-making approach utilizing a PC platform and LabVIEW application is employed in this study.

The work of Bondyra et al. [5] presented a prototype of a diagnostic system designed to detect and diagnose damaged rotary wing UAV blades. Acoustic emission data were collected by an onboard microphone array in conjunction with a small but powerful single-board computer based on a data-driven strategy that uses an artificial neural network to categorize auditory signal characteristics. Mel Frequency Spectrum Coefficients are used to generate fault signatures where a detailed assessment of the model's parameters was undertaken. The finest models not only identify fault occurrences but also indicate the position of the faulty rotor using multichannel data given by a microphone array resulting in high-accuracy classification. Moreover, Bondyra et al. [6] reported a failure detection technique for multirotor UAV propeller deficiencies where a developed program analyzed signal matrices from a network of accelerometer sensors near the propulsion units. MEMS accelerometers are used to quantify axial and radial vibrations, which offer data for feature extraction using the Fast Fourier Transform (FFT). The results revealed that identifying and isolating defective rotor states has a tremendous sensitivity.

In addition, the work of Bondyra et al. [7] provided a technique for detecting the physical deterioration of UAV rotor blades. A three-stage strategy based on signal processing and machine learning to identify rotor faults and assess their magnitudes and types as imbalanced rotating components typically create vibrations in mechanical systems, the approach is based on acceleration readings from the onboard IMU (Inertial Measurement Unit) sensor. This article examines three alternative techniques of feature extraction, as well as variable buffer length analysis. The provided solution was validated via several tests that demonstrated its efficacy utilizing a signal processing-based technique which was exceedingly adaptable and straightforward to incorporate into any flight controller. Furthermore, The work of Yoon et al. [8] offered an experimental assessment of hybrid fault detection and isolation strategy in skew-configured inertial sensors of an unmanned aerial vehicle against three subsequent failures employing FFT. A parity space technique and an in-lane monitoring approach were coupled to enhance system tolerance to several subsequent faults during flight. The parity space approach detects and isolates the first and second defects. Other methods, unlike FFT, were also utilized in terms of fault diagnosis of UAVs. To validate the performance of the proposed defect diagnostic approach, hardware-in-the-loop testing and flight experiments with a fixed-wing UAV were carried out.

Regarding recently published review papers that discuss the fault diagnosis of UAVs, the authors of Puchalski et al [9] are concerned about recent research on defect detection in UAVs. Fourlas et al [10] presented a complete review of current achievements and investigations in fault diagnosis, fault-tolerant control (FTC), and UAV anomaly detection. In terms of fault diagnosis of UAVs, the authors have also concluded that we are primarily interested in sensors and actuators since these subsystems are mostly subjected to failure, and their proper functioning typically ensures the smooth and dependable operation of the aerial vehicle. In addition to the previously mentioned survey article, many other surveys [11,12,13,14] have concluded that there is still to add in this field, especially in real-time approaches.

As previously noted, Section 1 of this paper served as an introduction to the used approach. It offered work related to the chosen method in the same research subject in addition to presenting novelty. Section 2 discusses the theoretical foundation using the Fast Fourier Transform (FFT), whereas Section 3 explains the experimental setup and sensor selection criteria. Section 4 discusses the findings, while Section 5 gives the conclusions of these findings.

Many research articles' primary flaw in observing UAV unit conditions and constraints is that they diagnose the multirotor UAV status at a specific time without considering the impact of cumulative faults, like a postponement in motor reaction times, adjustments in parameters in the early stages of a failure, or a change in the smoothness of the reaction to a climb, as the majority of intelligent drones are manufactured with a fault-avoiding system. Signal processing literature lacks real-time algorithms. Thus, the innovations and contributions of this research's surveillance and unbalance classification methodology are as follows:

- Describe the primary drawbacks of current research on multirotor UAV condition monitoring.
- Implement a fast Fourier transform method in real-time for monitoring UAV vibration signals.
- Quantifying defect and pre-failure probability over an extended period to generate an appropriate accumulation representation of requirements taking cumulative fault effect into account.
- Introducing a versatile and risk-free experimental method for collecting multirotor UAV vibration data which can also be adopted by any UAV of choice.

2. Theoretical Basis

The method of evaluating time-domain data is often used to check the health of various mechanical systems. It is determined by calculating statistics such as the root mean square (RMS), crest factor, standard deviation, variance, and peak-to-peak values [15,16]. The frequency-domain or spectrum analysis method is most frequently employed for rotary machine defect diagnostics. The time-domain vibration data are transformed into discrete frequency components using a frequency-domain signal processing technique that utilizes the fast Fourier transform (FFT) [17,18] To detect specific frequency components, the approach that operates in the frequency domain is preferred to the one that works in the time domain. In depicting the frequency spectrum, the X-axis represents frequency, and the Y-axis represents signal amplitude. However, signal representation within the time domain is not optimal in most applications since most critical information is concealed in the signal's frequency content. Frequency or spectrum analysis adds further information to time series data and may be used to understand the frequency spectra inside the signal. In damage detection, frequency domain analysis parameters are more trustworthy than time domain parameters. However, using Fourier transforms, a family of complex exponents may represent time-amplitude signals with indefinite duration. Furthermore, using Fourier transformations, every given time-domain signal may be expressed as a function of all its frequencies.

This is accomplished by dividing a signal x(t) into sinusoidal components of indefinite temporal length [19], which are provided by:

$$X(\omega) = \int_{-\infty}^{\infty} x(t)e^{-j\omega t}\, dt \quad (1)$$

where X(ω) is the converted signal, ω is the radian wavelength frequency, and t denotes the time. An inverse Fourier transform must be used to regenerate the time domain signal x(t) from the frequency domain signal X(ω):

$$X(t) = \frac{1}{2\pi}\int_{-\infty}^{\infty} x(\omega)e^{-j\omega t}\, d\omega \quad (2)$$

The continuous-time Fourier transform must only be applied to signals of infinite length and continuous time. Furthermore, since signals are usually recorded and stored digitally as a series of data points in most applications, the discrete Fourier transform (DFT) [20] is required, which is represented by:

$$\mathrm{X[k]} = \frac{1}{N}\sum_{n=0}^{N-1} \mathrm{x[n]e}^{-\mathrm{jk}(\frac{2\pi}{N})\mathrm{n}} \quad (3)$$

where X[k] and X[n] indicate the discrete frequency and time signals, k and n are the frequency and time indices, and N denotes the number of points evenly spaced in the range 0 to 2π..

3. Experimental Approach

3.1 Sensor Selection

Some problematic situations are hard to observe or uncover with the human eye, even after the drone inspection procedure has been completed; hence, the research of Ghazali et al [19] proposed a real-time early drone inspection technique based on vibration data. First, the detection reliability of many microelectromechanical systems (MEMS) sensors, including the ADXL335 accelerometer shown in Figure 1 below, the ADXL345 accelerometer, ADXL377 accelerometer, and SW420 vibration sensor, were examined and compared. Compared to other MEMS sensors, the testing findings revealed that the vibration parameter measured using ADXL335 and ADXL345 accelerometers is the best option since most defective circumstances can be recognized. The anomaly inspection algorithm's result is then translated to a "Healthy" or "Faulty" condition, presented in a mobile application for convenient monitoring. Because the ADXL335 is widely available in the market, particularly in the Iraqi industry, it was selected and employed in this investigation.

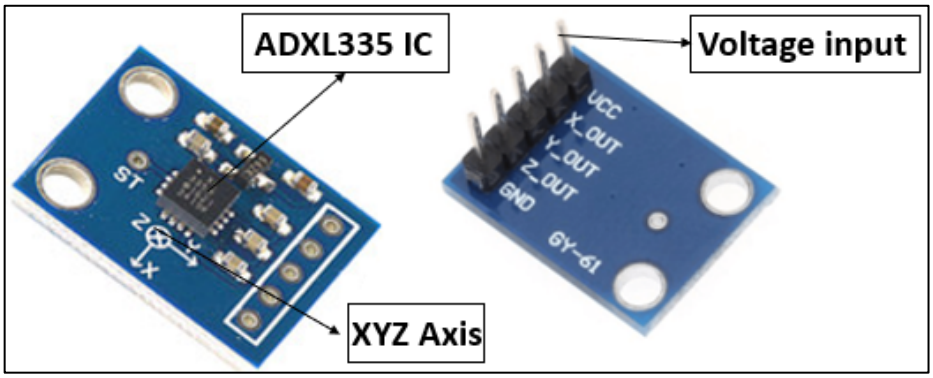

Figure 1: ADXL335 GY-61 accelerometer

3.2 Methodology

The DJI mini 2 combo [21,22] was selected as the small UAV because of its availability in the Iraqi market and affordable cost. The drone appears as seen in Figures 2 and 3. The damaged blades are located in the upper and lower right corners. This is owing to the left-side wire connections and, therefore, the right-side operability. The broken edges are demonstrated in Figure 2a, which shows the actual events when a drone collided with a tree. Figure 2b displays the construction of the instruments utilized in this investigation, as well as the position of the accelerometer. The accelerometer is attached to the drone at the intersecting lines of the four brushless motors; it is fixed in a manner where the drone pitches about the Y-axis, rolls about the X-axis, and yaws about the Z-axis. The ADXL335 is then linked to an NI DAQ 6009 (specifications shown in Table 1 below) and a PC platform represented by a Lenovo core i7 laptop, where the LabVIEW software is launched, and data are acquired. First, healthy measurements were gathered using the time-domain signals depicted in Figure 2, and then FFT was used to transform these into frequency-domain signals. Second and third, the damaged blade was used in place of the healthy blade, as explained in the previously mentioned positions. The time domain signals were gathered, while the frequency domain signals were converted using FFT, which will be briefly addressed in the next section. The theoretical section extends the analytical

background of the article and develops a new formulation of the problem. Calculations are achieved here using the developed equations and the modifications should be pointed out.

Table 1: DAQ-6009 Specifications

No.	Specifications	Information
1	Dimensions without connectors	63.5 mm × 85.1 mm × 23.2 mm
2	Weight With connectors	84 g
3	Maximum AI sample rate	48 kS/s
4	Operating Temperature	0 to 55°C
5	Analog Input Resolution	14 bits differential, 13 bits single-ended
6	Analog Output Resolution	12 bits

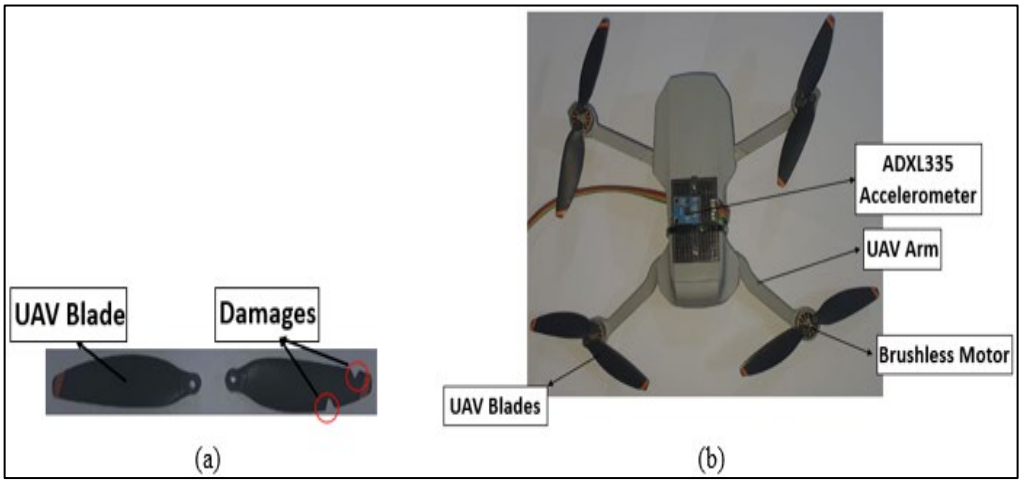

Figure 2: Experimental setup. (a) Damaged blades (b) location of ADXL335 on the drone

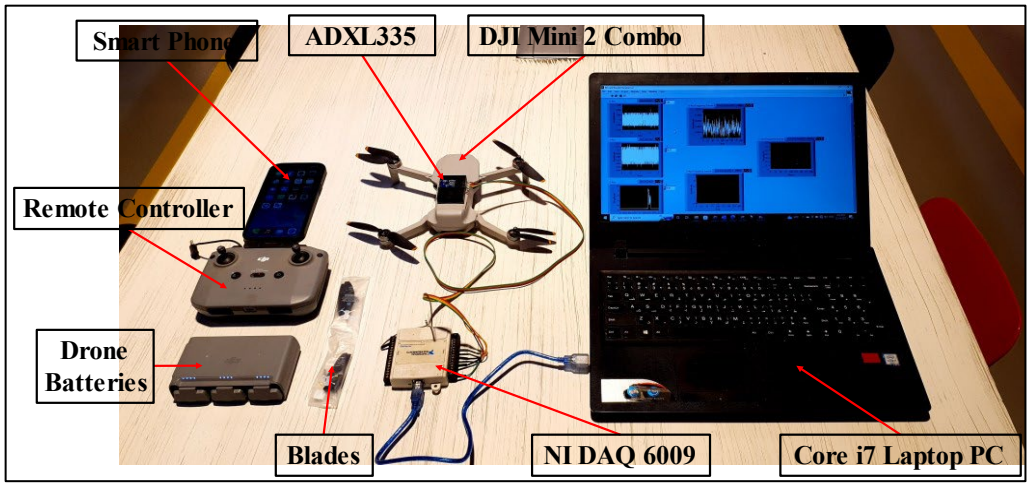

Figure 3: Experimental setup

3.3 Data Acquisition Based on LabVIEW Program

A sample block diagram of the prepared LabVIEW software is provided in Figure 4. Using the DAQMax LabVIEW add-on, the DAQ assistant option is added to LabVIEW, where the three-axis voltage inputs are established. With a frequency range of 1,000 Hz, a sample size of 2,000 is used for improved vibration signal representation. The signal is then split by the sensor's sensitivity and separated into three signals X, Y, and Z. Average of the arithmetic mean is then determined using Equation 4 below. N is the total number of samples, and Xi is the accelerations samples employed for calibration as a control subtraction. For the FFT to perform a spectrum analysis on a single signal, the graphs of all three axes must be identified and then combined. The signals are then split once again to depict each axis individually.

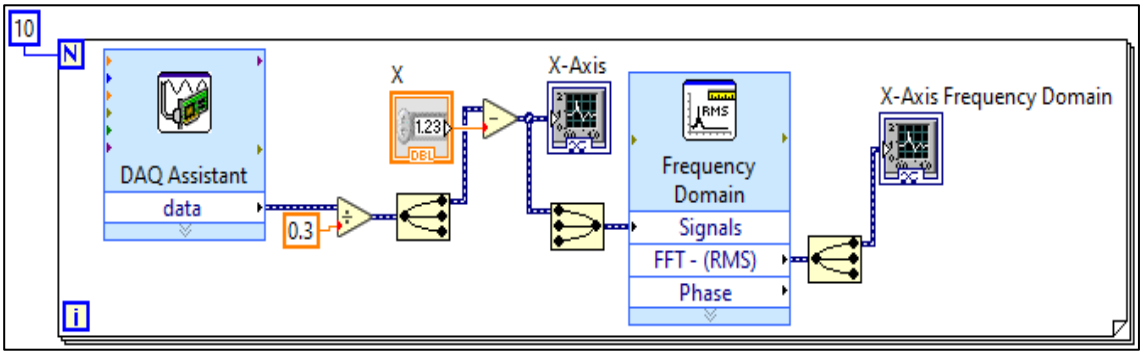

Figure 4: Sample of the total work signal processing block diagram

$$Arithmetic\ Mean = \frac{1}{N}\sum_{i=1}^{N} X_i \quad (4)$$

4. Results and Discussion

Figure 5 presents the studied 3 cases where Table 2 lists their boundary conditions. All have operated at hover mode with a constant motors' rpm of 10,000 RPM.

Table 2: Studied cases

Case	Hovering Speed (RPM)	Hovering Speed (Hz)	Location of Damaged Blade
Healthy	10,000	168	Nil
Blade 1 Damaged			Bottom Right
Blade 2 Damaged			Top Right

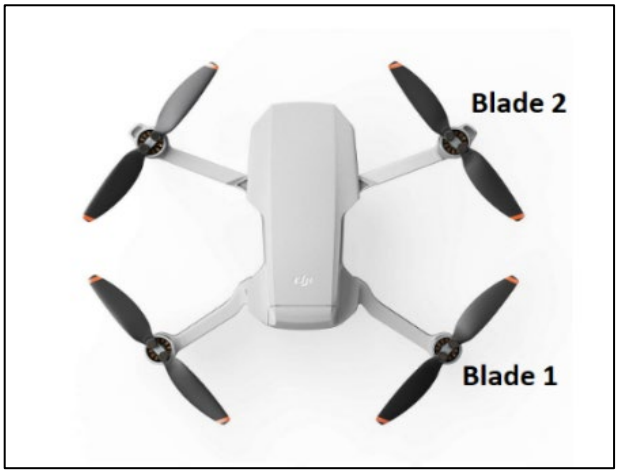

Figure 5: Blades' locations

When a healthy operational condition is evaluated, Figure 6 (a,b,c) illustrates the vibration signals in the time domain. The horizontal axis represents time in one-second total intervals, while the vertical axis represents the amplitude jump in acceleration units of meters per second squared. Signals along the X-axis have the most significant acceleration due to the influence of rolling, which has the most significant effect on vibration compared to pitching and yawing. Figures 7 and 8 (a,b,c) depict the time-domain vibration signals for the two analyzed cases, the first damaged blade, and the second damaged blade, respectively. Regardless of the location of the damaged blade, the rolling effect continues to exert the most considerable influence on the vibration pattern since larger amplitudes were observed in every case studied. Comparing the vibration graphs of the rolling state in three analyzed cases reveals that the amplitudes of the fault cases slightly exceed those of the healthy status, indicating the presence of a defect or an unhealthy operational condition. Comparing the signals reveals massive interference, from which it can be inferred that an instantaneous choice can be made based on the figures alone. Due to the fact that faulty operational situations produce signals with a similar pattern, it was deemed necessary to apply FFT for frequency-domain signals.

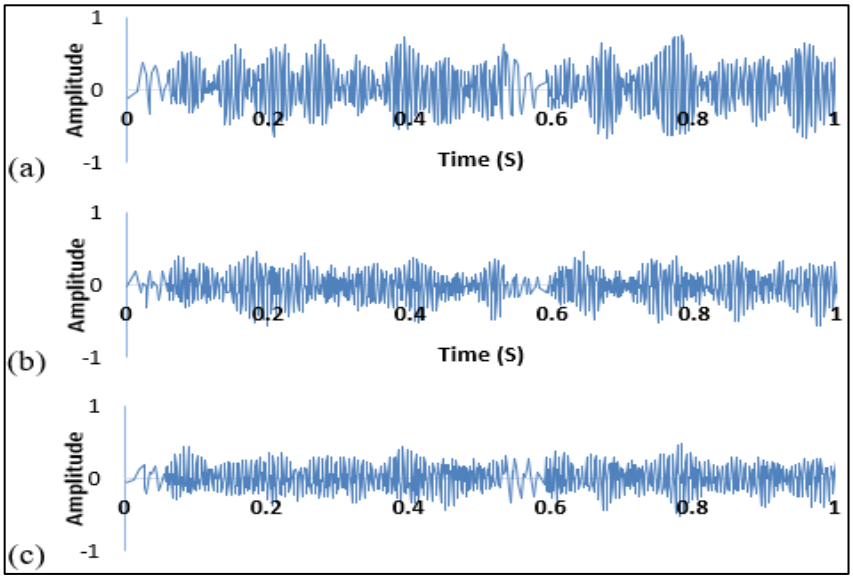

Figure 6: Vibration signals of healthy operating status in (a) X, (b) Y, and (c) Z axis

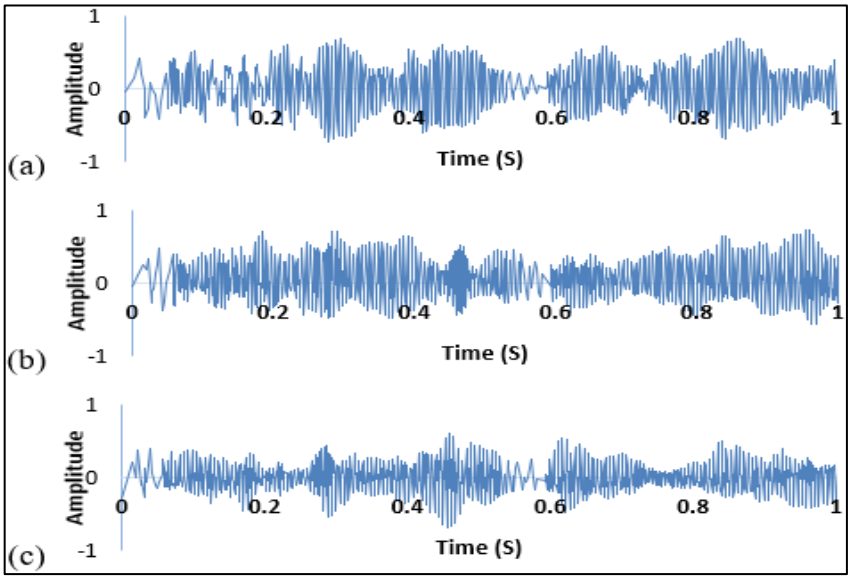

Figure 7: Vibration signals of the damaged blade one status in (a) X, (b) Y, and (c) Z axis

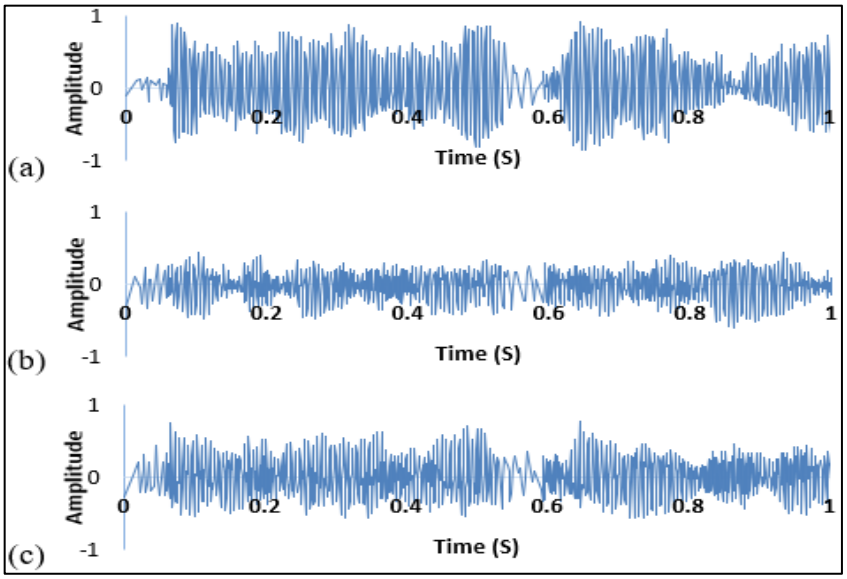

Figure 8: Vibration signals of damaged blade two status in (a) X, (b) Y, and (c) Z axis

As the time-domain vibration signals proved earlier, the X-axis vibration signals are of higher effect and more robust than the Y and Z axes. This is because vibration has a more significant impact on rolling movement than on pitching and yawing. Figure 9a depicts the frequency domain of the vibration signals in the X-axis where the drone rolls. It can be observed that the healthy readings have a maximum peak at roughly 166 Hz, which is the operating hover speed of the drone. When blade 1 is damaged, the peak shifts to the left with a new value of 163 Hz, and thus when blade 2 is damaged, the peak shifts to the left again but with a new value of 164 Hz. This is a strong indicator that an imbalance exists in the drone. Moreover, there is a disturbance where the drone tends to balance itself without faults at an operating speed of 172 Hz, where it can still be observed in the exact figure as a shorter peak. This value similarly shifts to the right with increased value in both damaged blade scenarios. Again, a solid indication of the presence of faults. Nevertheless, since both damaged cases are shifting the healthy readings toward one direction, it might be hard to locate the damaged case (blade), but easy to recognize the presence of a fault.When comparing the effect of yawing and pitching to that of rolling, a minor remark is made: rolling has a strong influence, while yawing and pitching have similar results. Figures 9b and 9c illustrate that frequency-domain vibration signals have a similar Y-axis and Z-axis presentation and are displayed accordingly. This means we may eliminate one of them to reduce the amount of data collected, manage time, and save energy effectively. In addition, to detect the damaged blade of the drone, the healthy readings of the Y-axis indicate a hovering speed peak of 166 Hz—the peak shifts to the right with a more excellent value of 173 Hz when blade1 is damaged. When blade 2 is broken, however, the peak moves to the left and has a lower value of 163 Hz. Regardless of the new peak values of the drone's brushless motors, the direction shift reveals the location of the damaged blade. When the value shifts to the right, this indicates that the damaged blade is 1 and hence at the bottom. When the value shifts to the left, this suggests that the damaged blade has a value of 2 and is consequently in the top position. The X-axis of the drone reveals whether an imbalance exists. The Y-axis, which indicates the drone's pitch, or the Z-axis, which marks its roll, reveals the location of the damaged blade. A complete system utilizing two axes of the vibration sensor is maintained to categorize imbalance in any operating drone. Moreover, it can be observed that more fluctuated amplitudes are occurring in the Z-axis for all operating statuses, especially when blade one is damaged. The Z-axis represents the drone when it moves in an elevated motion or descending movement. Blade 1 is located in the lower section of the drone where the unbalance is of greater impact on the overall performance. Hence, these noticed fluctuated amplitudes are due to the tendencies of the embedded system where the UAV tries to rebalance itself inducing higher and lower motor speeds, regardless of the operating motor.

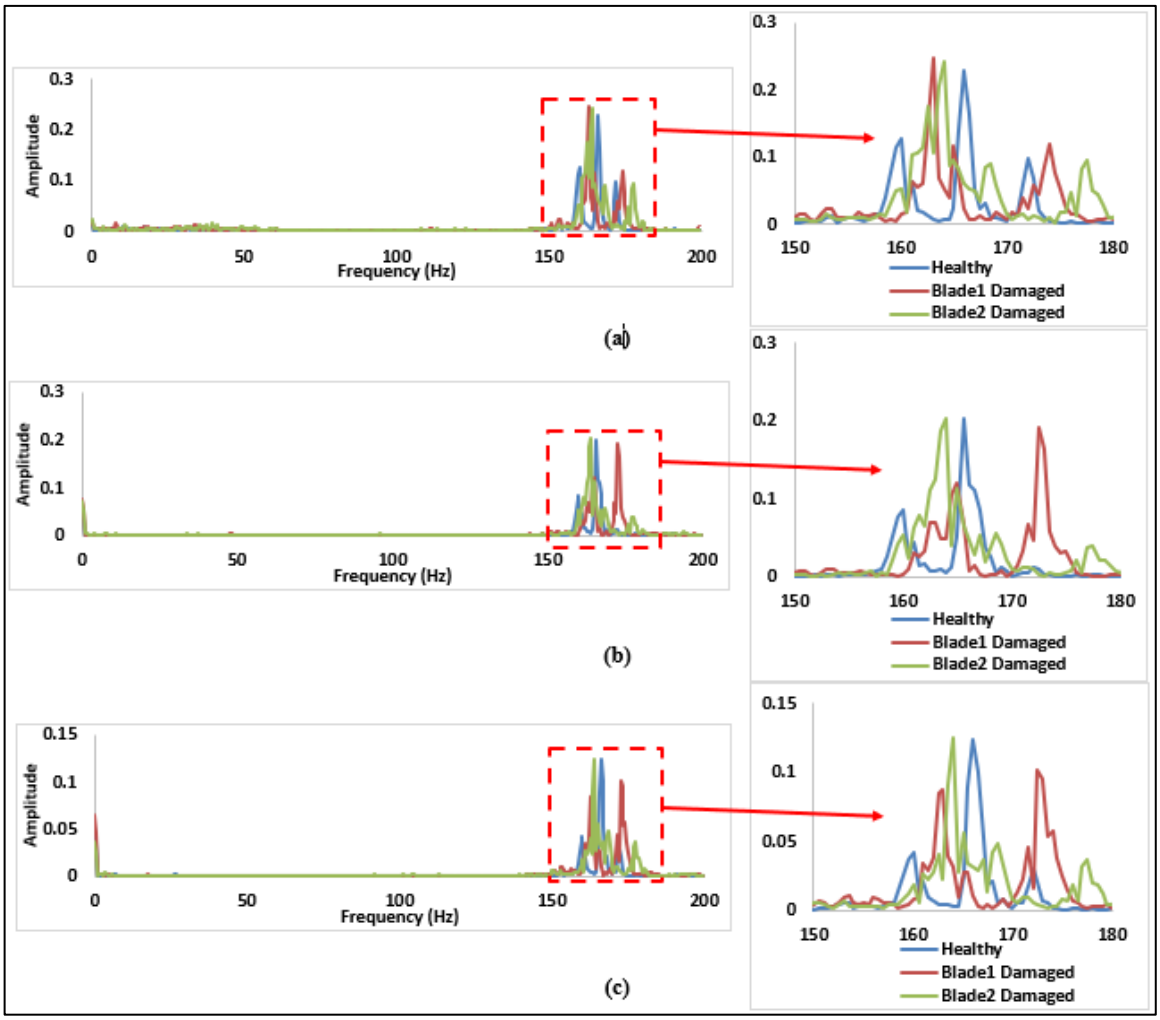

Figure 9: Frequency-domain analysis. (a) X-axis (b) Y-axis (c) Z-axis

As a result, the exhibited visuals in real-time disclose the presence of a malfunction by comparing the frequency-domain vibration signals to those of the healthy operational condition for unbalanced classification. Even though it may be challenging to determine the exact location of the damaged blade, the software graphs demonstrate indisputably that it exists. Table 3 enlists the max peak frequency in Hertz varying in all three studied cases of each axis. The shifting percentage is also presented regardless of the shifting direction. Interestingly, the Y axis proved reasonable reliance in determining the presence of a fault due to the highest shifting percentage. This table is for comparison purposes stating that real-time graphs are still of better indication of the presence of faulty flying modes regardless of the location of these faulty operational statuses.

Table 3: Peak frequency shifting percentages

Axis	Case Studies	Max Peak Frequency (Hz)	Shifting percentage (from the healthy state)
	Healthy	166	-
X	Damaged Blade 1	163	1.807%
	Damaged Blade 2	164	1.205%
	Healthy	165.5	-
Y	Damaged Blade 1	172.5	4.23%
	Damaged Blade 2	164	0.906%
	Healthy	166	-
Z	Damaged Blade 1	172.5	3.916%
	Damaged Blade 2	164	1.205%

5. Conclusion

Based on vibration signal analysis, this study developed an experimental technique to evaluate a commercial drone unbalanced classification system. Several studies were carried out to assess the influence of altering blade health on the intensity of drone vibration. The simulated blade defects were considered damage down the blade's length. The considered NI 6009 DQA and LabVIEW software offered real-time unbalanced classification. Vibration-based condition monitoring may uncover drone faults by monitoring time-domain and frequency-domain signal bandwidths utilizing FFT.

The frequency spectrum can be investigated using the fast Fourier transform in real-time. The vibration signal spectrum, in particular, may uncover drone flaws. When the drone is healthy, the feature amplitudes are modest, but they are the largest and most disturbed when defects are simulated. High vibration amplitudes result from the damaged blades influencing unbalances. As a consequence, the broken blades have an impact on the total vibration level of the drone system.

However, more UAV equipment is necessary to establish the external sensor network. Furthermore, the UCI system's reaction time is mainly determined by the time of signal acquisition. As a result, there is a considerable delay between the incidence of the defect and the receipt of diagnostic information—the application of the proposed FDI system to any multirotor needs a classifier training procedure. More studies will be conducted to fine-tune the approach, reduce the needed data-collecting time, and build the fault detection system with the associated fault-tolerant control scheme. In addition, an intelligent system based on machine learning approaches, such as artificial neural networks, is suggested to identify different drone issues for future work.

Acknowledgment

The authors would like to acknowledge the help provided by the cited researchers.

Author Contribution

Conceptualization, A. Jaber.; methodology, A. Jaber.; software, S.A.; validation, L.A.; formal analysis, L.A.; investigation, L.A.; writing—original draft preparation, L.A.; writing—review and editing, L.A., A.J., and P.N.; supervision, A.J.; project administration, A.J. All authors have read and agreed to the published version of the manuscript

Funding

This research received no external funding.

Data Availability Statement

The researcher took the information, and the rest of the data is in the author's thesis in the Department of Mechanical Engineering, University of Technology Library.

Conflicts of Interest

The authors declare no conflict of interest.

References

[1] B. Alzahrani, O. S. Oubbati, A. Barnawi, M. Atiquzzaman, D. Alghazzawi, UAV assistance paradigm: State-of-the-art in applications and challenges, J. Network Comput. Appl.,166 (2020) 102706. https://doi.org/10.1016/j.jnca.2020.102706

[2] A. Abdulkareem, A. Humod, O. Ahmed, Fault Detection and Fault Tolerant Control for Anti-lock Braking Systems (ABS) Speed Sensors by Using Neural Networks, Eng. Technol. J., 41 (2022) 1–12. http://doi.org/10.30684/etj.2022.135106.1259

[3] S. Jawad and A. Jaber, Bearings Health Monitoring Based on Frequency-Domain Vibration Signals Analysis, Eng. Technol. J., 41 (2022) 86–95. http://doi.org/10.30684/etj.2022.131581.1043

[4] K. Jalal, L. Abd alameer, Fault Diagnosis in Wind Power System Based on Intelligent Techniques, Eng. Technol. J., 36 (2018)1201–1207. https://doi.org/10.30684/etj.36.11A.11

[5] A. Bondyra, M. Kołodziejczak, R. Kulikowski, W. Giernacki, An Acoustic Fault Detection and Isolation System for Multirotor UAV, Energies (Basel), 15 (2022) 3955. https://doi.org/10.3390/en15113955

[6] A. Bondyra, P. Gasior, S. Gardecki, A. Kasinski, Development of the Sensory Network for the Vibration-based Fault Detection and Isolation in the Multirotor UAV Propulsion System, in ICINCO 2018 - Proceedings of the 15th International Conference on Informatics in Control, Automation and Robotics, 2 (2018) 102–109. https://doi.org/10.5220/0006846801020109

[7] A. Bondyra, P. Gasior, S. Gardecki, A. Kasiński, Fault diagnosis and condition monitoring of UAV rotor using signal processing, in 2017 Signal Processing: Algorithms, Architectures, Arrangements, and Applications, (2017) 233–238. https://doi.org/10.23919/SPA.2017.8166870

[8] S. Yoon, S. Kim, J. Bae, Y. Kim, E. Kim, Experimental evaluation of fault diagnosis in a skew-configured UAV sensor system, Control. Eng .Pract., 19 (2011) 158–173. https://doi.org/10.1016/j.conengprac.2010.11.004

[9] R. Puchalski, W. Giernacki, UAV Fault Detection Methods, State-of-the-Art, Drones, 6 (2022) 330. https://doi.org/10.3390/drones6110330

[10] G. K. Fourlas, G. C. Karras, A survey on fault diagnosis and fault-tolerant control methods for unmanned aerial vehicles, Machines, 9 (2021) 197. https://doi.org/10.3390/machines9090197

[11] G. K. Fourlas, G. C. Karras, A Survey on Fault Diagnosis Methods for UAVs, in 2021 Inte. Conf. Unmanned Aircraft Syst., (2021) 394–403. https://doi.org/10.1109/ICUAS51884.2021.9476733

[12] I. Sadeghzadeh, Y. Zhang, A Review on Fault-Tolerant Control for Unmanned Aerial Vehicles (UAVs), in Infotech@Aerospace 2011, American Institute of Aeronautics and Astronautics, 2011. https://doi.org/10.2514/6.2011-1472

[13] D. Li, Y. Wang, J. Wang, C. Wang, Y. Duan, Recent advances in sensor fault diagnosis: A review, Sens. Actuator A Phys., 309 (2020) 111990. https://doi.org/10.1016/j.sna.2020.111990

[14] H. Shraim, A. Awada, R. Youness, A survey on quadrotors: Configurations, modeling and identification, control, collision avoidance, fault diagnosis and tolerant control, IEEE Aerosp. Electron. Syst. Mag., 33 (2018) 14–33. https://doi.org/10.1109/MAES.2018.160246

[15] S. Xiang, L. Yang, Y. Wang, Robust and Reversible Audio Watermarking by Modifying Statistical Features in Time Domain, Adv. Multimedia., 2017 (2017) 1-10. https://doi.org/10.1155/2017/8492672

[16] M. M. Tahir, A. Q. Khan, N. Iqbal, A. Hussain, S. Badshah, Enhancing Fault Classification Accuracy of Ball Bearing Using Central Tendency Based Time Domain Features, IEEE Access, 5 (2017) 72–83. https://doi.org/10.1109/ACCESS.2016.2608505

[17] B. Li, Z. Jiang, J. Chen, Performance of the Multiscale Sparse Fast Fourier Transform Algorithm, Circuits Syst. Signal Process., 41 (2022) 4547–4569. https://doi.org/10.1007/s00034-022-01989-6

[18] P. Xia, H. Zhou, H. Sun, Q. Sun, R. Griffiths, Research on a Fiber Optic Oxygen Sensor Based on All-Phase Fast Fourier Transform (apFFT) Phase Detection, Sensors, 22 (2022). https://doi.org/10.3390/s22186753

[19] M. H. M. Ghazali, W. Rahiman, An Investigation of the Reliability of Different Types of Sensors in the Real-Time Vibration-Based Anomaly Inspection in Drone, Sensors, 22 (2022) 6015. https://doi.org/10.3390/s22166015

[20] Sundararajan, D. (2023).The Discrete Fourier Transform, in Signals and Systems: A Practical Approach, D. Sundararajan, Ed. Cham: Springer Nature Switzerland, pp 125–160. https://doi.org/10.1007/978-3-031-19377-4_5

[21] M. Stanković, M. M. Mirza, U. Karabiyik, UAV forensics: DJI mini 2 case study, Drones, 5 (2021) 49. https://doi.org/10.3390/drones5020049

[22] L. A. Al-Haddad, A. A. Jaber, An Intelligent Fault Diagnosis Approach for Multirotor UAVs Based on Deep Neural Network of Multi-Resolution Transform Features, Drones, 7 (2023) 82. https://doi.org/10.3390/drones7020082